

Fuzzy pid controller design and simulation of brake by wire system based on giant -magnetostrictive material

CHANGBAO CHU², XINGJIAN JIA², YUE XIAO²,
YUPING ZENG²

Abstract. Brake by wire system has great significance to improve vehicle active safety. The paper takes brake by wire system that is using giant -magnetostrictive material as the research object. On the basis of establishing its mathematical model, fuzzy PID controller was designed and compared with the PID controller. Simulation results show that the system can meet the braking requirements. Compared with PID control algorithm, amplitude of slip ratio that is using fuzzy logic PID control algorithm fluctuates smaller. Slip ratio is precisely controlled nearby 0.2. Braking distance is shortened about 1.3 m compared with braking distance that is using PID control algorithm. Vehicle's active safety performance is improved.

Key words. Giant-magnetostrictive material, brake by wire, control, automobile.

1. Introduction

Brake by wire system (abbreviation BBW) has great significance to improve vehicle active safety. It is the development direction of automobile electronic control brake system.

Hardware-in-the-Loop was used to evaluate the performance of electronic wedge brake actuator in controlling the gap and torque^[1–2]. The fail-safe control strategies of brake by wire system was proposed by Jeon, Kwangki for improvement in the straight braking stability^[3]. Hwang, Woohyun proposed fault detection and estimation for electromechanical brake systems using parity space approach^[4]. Pedal

¹Acknowledgement - Education department of Jiangxi province under Grant No. GJJ14746 and Jiangxi Province Key Laboratory of Precision Drive & Control, Nanchang Institute of Technology under Grant No. PLPDC-KFKT-201618 sponsored this paper, the authors deeply appreciate the supports.

²Jiangxi Province Key Laboratory of Precision Drive & Control, Nanchang Institute of Technology, Nanchang, China; e-mail: chuchangbao@163.com

simulator and braking feel evaluation in brake by wire system were carried out by Ji, Fenzhu and Zhu, Wen Bo^[5-6]. Leiyan, Yu established dynamics model of brake by wire system and analyzed the time domain and frequency domain response characteristics^[7]. Haggag, Salem A. Proposed an optimal control tracking strategy for brake by wire system and tested on a laboratory setup^[8]. Optimization and robust design was carried out by Kwon, Yongsik for the electronic wedge brake caliper and the pedal simulator^[9]. An asymmetric dual-core architecture with an external watchdog processor was introduced to implement functional safety-oriented monitoring functions for brake by wire system^[10]. Most studies on brake by wire system take motor as braking power. Because the motor often works in locked conditions, the work reliability of the motor demand is higher. Enforcement agencies generally consist of planetary gear reducer and ball screw, the structure significantly increased the complexity of the actuator and assembly costs. At the same time, because of the existence of transmission mechanism, increase the braking system response time of the actuator. Based on above reasons, the EMB in active safety performance remains to be further improved.

2. System Structure and Vehicle Dynamic Model

2.1. System Structure

As the driving source, the GMM rod generates axial displacement under magnetic field and pushes another end of the compliant mechanism brake disc to realize brake on both sides of brake disc. System structure is shown in figure 1.

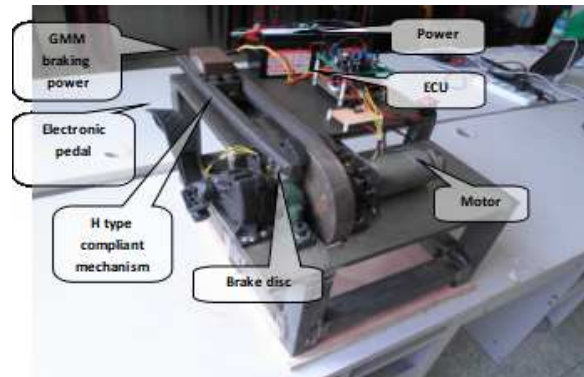


Fig. 1. Structure of braking system

2.2. Vehicle Dynamic Model

Three DOF of vehicle model is considered. Longitudinal motion equation

$$\delta (V_1 - \lambda^2 T_1) = 0, \quad (1)$$

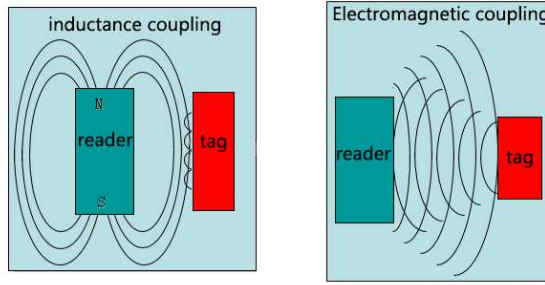


Fig. 2. Vehicle model

Rotary motion equation

$$T = \frac{ab}{2} \rho_0 h_0 \omega^2 \int_A p_1 p_2 \left[1 - (1 - \beta) \left(\xi + \frac{1}{2} \right)^2 \right] w^2 dA, \quad (2)$$

$$V = \frac{ab}{2} \frac{E_0 h_0^3}{12(1 - \nu^2)} \int_A (p_1 p_2)^3 p_3 (G - 2(1 - \nu)H) dA \quad (3)$$

adhesive force

$$F_{x1} = u_x F_{z1} \quad (4)$$

$$F_{x2} = u_x F_{z2} \quad (5)$$

m : vehicle mass, v : acceleration, F_{xi} : adhesive force, R_i : rolling radius, u_x : adhesion coefficient, J_ω : rotational inertia, ω_i : angular velocity, $F_z F_{zi}$: normal reaction, M_i : braking torque ($i=1,2$).

2.3. Brake Model

GMM actuator displacement output characteristic refers to the relationship between input current and output displacement. Under the condition of considering thermal deformation, GMM rod axial magnetostriction constitutive equation as follows:

$$\varepsilon_3 = s_{33}^H \sigma_3 + d_{33} H_3 + \alpha_{33} \Delta T \quad (6)$$

$$B_3 = d_{33} \sigma_3 + u_{33}^\sigma H_3 \quad (7)$$

GMM actuator output force f is equal to the product of axial stress and the

equivalent sectional area. Output force f shows as follows.

$$f = -A_3\sigma_3 = \frac{-A_3}{S_{33}^H} \left\{ \frac{\Delta l}{l_3} - \alpha_{33}\Delta T - d_{33}[(NI)_{actu}/(u_3A_3 \sum_{i=1}^3 R_{Mi}) + H_{bias}] \right\} \quad (8)$$

If other parameters are determined, actuator output force f is only relevant to input current I and GMM rod strain $\Delta l/l_3$. if $\Delta l=0$, the biggest potential output force of GMM rod can be calculated as follows.

$$f_{\max} = \frac{A_3}{S_{33}^H} \left\{ \alpha_{33}\Delta T + d_{33}[(NI)_{actu}/(u_3A_3 \sum_{i=1}^3 R_{Mi}) + H_{bias}] \right\} \quad (9)$$

Formulas (3, 4) express the relationship of static function between input current and the GMM actuator output force . Because the GMM rod usually maintains expansion amount near the largest displacement during braking process, maximum displacement ($\Delta l = 280\mu m$) is adopted during debugging process.

According to formulas of (8, 9), the whole system brake model shows as follows.

$$M = \frac{-f' A_3 r}{S_{33}^H} \left\{ \frac{\Delta l}{l_3} - \alpha_{33}\Delta T - d_{33}[(NI)_{actu}/(u_3A_3 \sum_{i=1}^3 R_{Mi}) + H_{bias}] \right\} \quad (10)$$

s_{33}^H : Longitudinal flexibility coefficient at constant magnetic field, σ_3 : axial stress, d_{33} : The axial dynamic magnetostrictive coefficient, α_{33} : coefficient of thermal expansion, ΔT : temperature rise, A_i : equivalent sectional area, I :exciting current, N :number of turns, l_i :length of a magnetic pat, u_i :Material permeability, R_{Mi} :magnetic resistance, H_{bias} :bias magnetic field strength.subscript $i=1,2,3$, respectively stands for ferromagnetic material, air gap and GMM rod. M :braking torque f' :coefficient of friction r :Brake disc radius. Parameters and values can be find in reference.

3. Fuzzy PID Controller Design

3.1. Fuzzy of Input and Output

Take slip rate error e and slip rate of error change rate ec as the controller inputs, take the variation of parameters K_p, K_i , and K_d as controller outputs. Fuzzy sets of e and ec are as follows: {NB,NM,NS,ZO,PS,PM,PB}, domain of discourse of e and ec are as follows: {-3,-2,-1,0,1,2,3}. Both of them obey the triangle membership function curve. The input membership functions(abbreviation:imf) are shown in figure 3 and figure 4. Fuzzy sets of K_p, K_i , and K_d are as follows: {NB,NM,NS,ZO,PS,PM,PB}, domain of discourse of K_p, K_i , and K_d are as follows: {-3,-2,-1,0,1,2,3}. All of them obey the triangle membership function curve. The output membership functions are shown in figure 5-7.

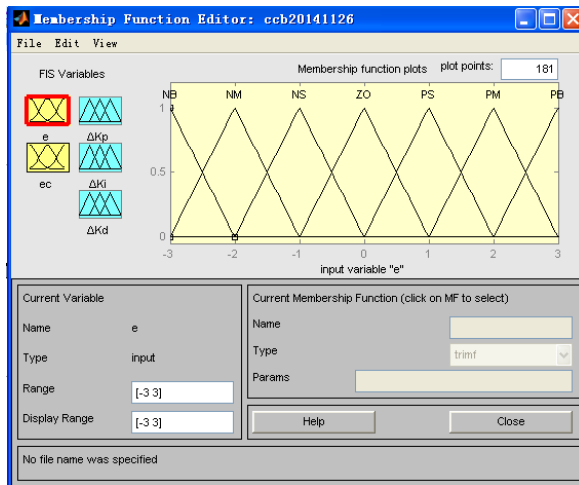


Fig. 3. Imf of slip rate error

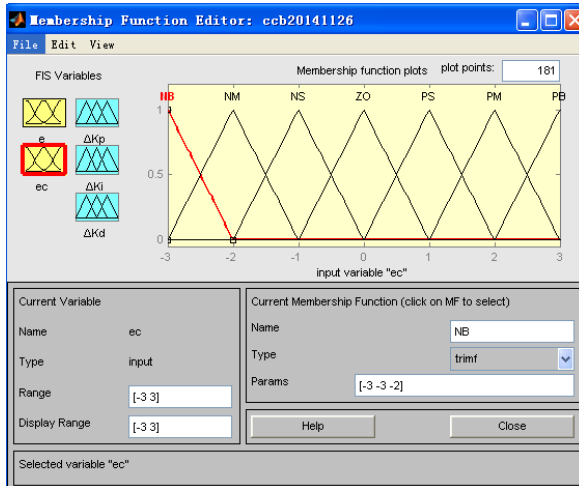


Fig. 4. Imf of slip rate of error change rate

Table 1. ΔKp fuzzy rules

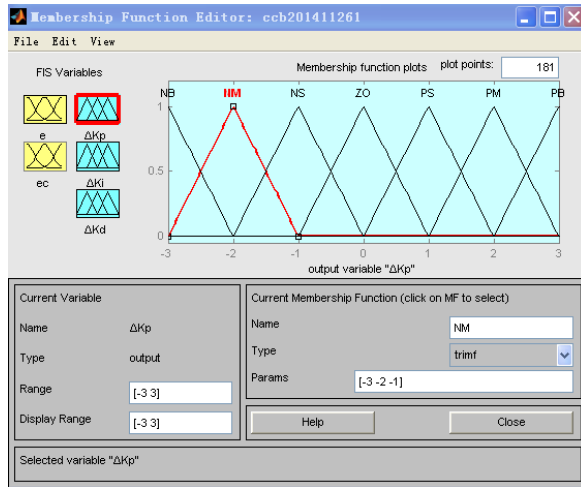


Fig. 5. Output membership function of K_p

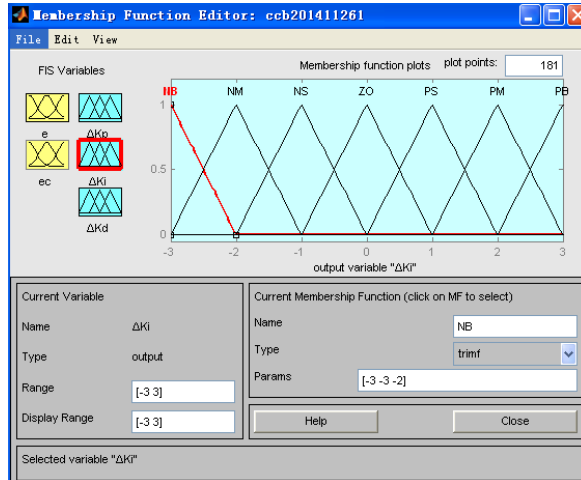


Fig. 6. Output membership function of K_i

ΔK_p		EC							
		NB	NM	NS	ZO	PS	PM	PB	
E	NB	PB	PB	PM	PM	PS	ZO	ZO	
	NM	PB	PB	PM	PS	PS	ZO	NS	
	NS	PM	PM	PM	PS	ZO	NS	NS	
	ZO	PM	PM	PS	ZO	NS	NM	NM	
	PS	PS	PS	ZO	NS	NS	NM	NM	
	PM	PS	ZO	NS	NM	NM	NM	NB	
	PB	ZO	ZO	NM	NM	NM	NB	NB	

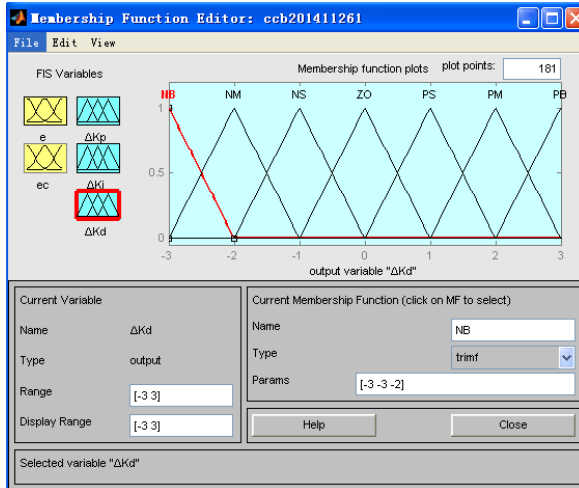


Fig. 7. Output membership function of ΔKd

3.2. Fuzzy control rule table

K_p , K_i , K_d are respectively proportion coefficient, integral and differential coefficient. According to the parameters (K_p , K_i , K_d) influence to output characteristic, requirements of parameters self-tuning are as follows:

When $|e|$ is larger, in order to prevent differential supersaturation caused by instantaneous larger initial deviation, larger K_p and smaller K_d should be adopted;

When $|e|$ and $|ec|$ are medium, smaller K_p should be adopted;

When $|e|$ is smaller, Integral element is effective, larger K_p and K_i should be adopted;

According to the parameter self-tuning principle, Fuzzy PID control rules table shown in the following tables.

Table 2. ΔK_i fuzzy rules

ΔK_i			EC						
			NB	NM	NS	ZO	PS	PM	PB
E	NB		NB	NB	NM	NM	NS	ZO	ZO
	NM		NB	NB	NM	NS	NS	ZO	ZO
	NS		NB	NM	NS	NS	ZO	PS	PS
	ZO		NM	NM	NS	ZO	PS	PM	PM
	PS		NM	NS	ZO	PS	PS	PM	PB
	PM		ZO	ZO	PS	PS	PM	PB	PB
	PB		ZO	ZO	PS	PM	PM	PB	PB

Table 3. Kd fuzzy rules

??Kd			EC						
			NB	NM	NS	ZO	PS	PM	PB
E	NB		PS	NS	NB	NB	NB	NM	PS
	NM		PS	NS	NB	NM	NM	NS	ZO
	NS		ZO	NS	NM	NM	NS	NS	ZO
	ZO		ZO	NS	NS	NS	NS	NS	ZO
	PS		ZO						
	PM		PB	NS	PS	PS	PS	PS	PB
	PB		PB	PM	PM	PM	PS	PS	PB

Using the MATLAB fuzzy logic toolbox provided by fuzzy inference system (FIS), the fuzzy controller that consists of two inputs and three outputs is established. As is shown in figure 8. Membership function of inputs and outputs are given by membership function editor. In the rule editor, according to the fuzzy control rules, 49 fuzzy control rules are established. As is shown in figure 9.

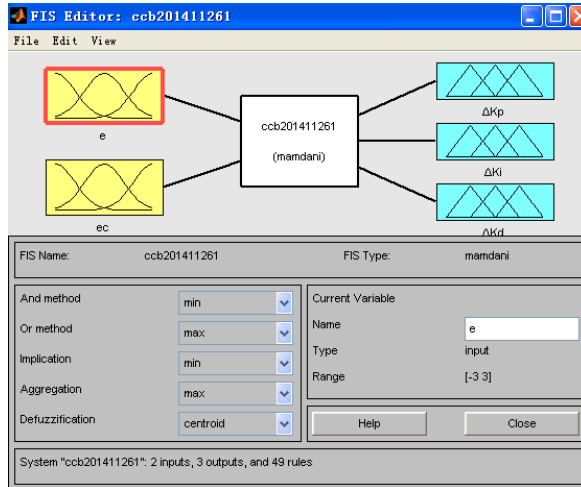


Fig. 8. Fuzzy inference system

4. Simulation and Results Analysis

Vehicle starting speed is 100 km/h. P=30, I=0.012, D=0. Let the vehicle brake on dry concrete pavement. The simulation results are shown in Fig 10 ~ Fig13.

Fig 10 shows that in the process of the brake, slip ratio maintained near the optimal slip ratio($s=0.2$), the adhesion coefficient maintained near the peak adhesion

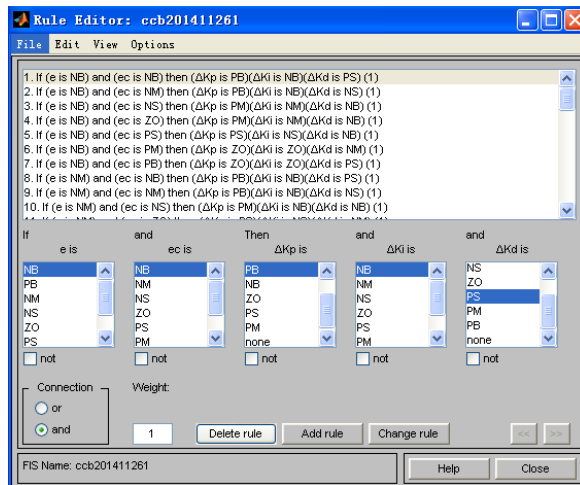


Fig. 9. Fuzzy control rules

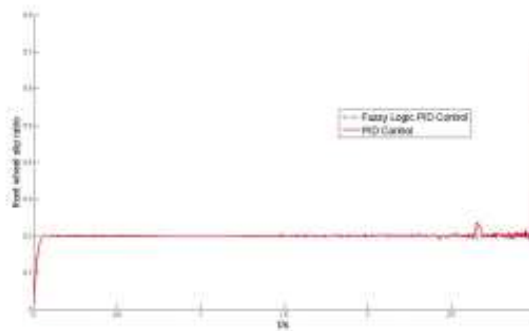


Fig. 10. Simulation curve of slip ratio

coefficient, so as to achieve the best braking effect. Compared with PID control algorithm, amplitude of slip ratio that is using fuzzy logic PID control algorithm fluctuates smaller. Slip ratio is precisely controlled.

Fig 10 shows that braking distance that is using fuzzy logic PID control algorithm is $43.4m$, braking distance is reduced about $1.3m$ compared with braking distance that is using PID control algorithm. The shortened braking distance is of great significance when emergency happens.

5. Conclusions

The paper takes brake by wire system that is using giant -magnetostrictive material as the research object. On the basis of establishing its mathematical model, fuzzy logic PID controller was designed and compared with the PID controller.

References

- [1] J. S. TOMAR, D. C. GUPTA, N. C. JAIN: *Model-in-the-Loop Simulation of gap and torque tracking control using electronic wedge brake actuator*. International Journal of Vehicle Safety 15 (1984), No. 2, 211–220.
- [2] J. S. TOMAR, A. K. GUPTA: *Study on the potential application of electronic wedge brake for vehicle brake system*. International Journal of Modelling, Identification and Control 98 (1985), No. 2, 257–262.
- [3] R. H. GUTIERREZ, P. A. A. LAURA: *Electronic brake safety index for evaluating fail-safe control of brake-by-wire systems for improvement in the straight braking stability*. Proceedings of the Institution of Mechanical Engineers, Part D: Journal of Automobile Engineering 18 (1985), No. 3, 171–180.
- [4] R. P. SINGH, S. K. JAIN: *Fault detection and estimation for electromechanical brake systems using parity space approach*. Journal of Dynamic Systems, Measurement and Control, Transactions of the ASME 7 (2004), No. 1, 41–52.
- [5] M. N. GAIKWAD, K. C. DESHMUKH: *Design and simulation of pedal simulator in brake by wire system*. Applied Mechanics and Materials 29 (2005), No. 9, 797–804.
- [6] S. CHAKRAVERTY, R. JINDAL, V. K. AGARWAL: *Modeling and analysis of brake by wire system in electric vehicle*. Applied Mechanics and Materials 12 (2005) 521–528.

Received November 16, 2016